




Secretory kinase Fam20C tunes endoplasmic reticulum redox state via phosphorylation of Ero1 α

Jianchao Zhang^{1,2} , Qinyu Zhu^{3,4}, Xi'e Wang^{1,2}, Jiaojiao Yu^{1,2}, Xinxin Chen^{1,2}, Jifeng Wang⁵, Xi Wang^{1,2}, Junyu Xiao^{3,4} , Chih-chen Wang^{1,2} & Lei Wang^{1,2,*} 

Abstract

Family with sequence similarity 20C (Fam20C), the physiological Golgi casein kinase, phosphorylates numerous secreted proteins that are involved in a wide variety of biological processes. However, the role of Fam20C in regulating proteins in the endoplasmic reticulum (ER) lumen is largely unknown. Here, we report that Fam20C interacts with various luminal proteins and that its depletion results in a more reduced ER lumen. We further show that ER oxidoreductin 1 α (Ero1 α), the pivotal sulfhydryl oxidase that catalyzes disulfide formation in the ER, is phosphorylated by Fam20C in the Golgi apparatus and retrograde-transported to the ER mediated by ERp44. The phosphorylation of Ser145 greatly enhances Ero1 α oxidase activity and is critical for maintaining ER redox homeostasis and promoting oxidative protein folding. Notably, phosphorylation of Ero1 α is induced under hypoxia, reductive stress, and secretion-demanding conditions such as mammalian lactation. Collectively, our findings open a door to uncover how oxidative protein folding is regulated by phosphorylation in the secretory pathway.

Keywords ER redox; Ero1 α ; Fam20C; oxidative protein folding; phosphorylation

Subject Categories Membrane & Intracellular Transport; Post-translational Modifications, Proteolysis & Proteomics

DOI 10.15252/emboj.201798699 | Received 22 November 2017 | Revised 20 April 2018 | Accepted 24 April 2018 | Published online 1 June 2018

The EMBO Journal (2018) 37: e98699

Introduction

Protein phosphorylation regulates almost every aspect of cell life, including the cell cycle, growth, differentiation, migration, and death, due to its simplicity, flexibility, and reversibility (Cohen, 2002). It is estimated that around 30% of human proteins are phosphoproteins. The first phosphoprotein, casein, was reported in 1883 (Hammarsten, 1883) and has been widely used as a model substrate to evaluate protein kinase activity, yet family with sequence

similarity 20C (Fam20C), the *bona fide* kinase catalyzing the phosphorylation of secreted protein casein, was not identified until 2012 (Ishikawa *et al*, 2012; Tagliabracci *et al*, 2012). Fam20C is a unique protein kinase that phosphorylates proteins within the S-x-E/pS motif, preferentially uses Mn²⁺ over Mg²⁺ as a metal ion cofactor and displays insensitivity to the broad-spectrum protein kinase inhibitor staurosporine (Tagliabracci *et al*, 2012).

Loss-of-function mutations in Fam20C cause a rare and often lethal osteosclerotic bone dysplasia called Raine syndrome (Raine *et al*, 1989). Indeed, Fam20C has been found to phosphorylate proteins important to biomineralization, including osteopontin, dentin matrix protein-1, and dentin sialophosphoprotein (Ishikawa *et al*, 2012; Tagliabracci *et al*, 2012). Recently, Dixon laboratory reported that Fam20C is the kinase responsible for generating the majority of the secreted phosphoproteome (more than 100 secreted proteins) implicated in a broad-spectrum of biological processes, such as wound healing, regeneration, and cell migration (Tagliabracci *et al*, 2015). This implies that Fam20C participates in a wide variety of regulations in human physiology and disease. However, little is known about the role of protein phosphorylation in the endoplasmic reticulum (ER) lumen.

More than 30% of the proteins encoded by the human genome are predicted to enter the secretory pathway (Fass & Thorpe, 2018). Most secreted and membrane proteins (e.g., cytokines, immunoglobulins, and receptors) contain disulfide bonds that stabilize their structures and regulates their functions (Hogg, 2003). The folding of nascent peptides accompanied by disulfide bond formation is called oxidative protein folding. The ER is the central organelle for secreted and membrane protein synthesis, folding, and assembly. The pivotal pathway for catalyzing oxidative protein folding in the ER is composed of sulfhydryl oxidase ER oxidoreductin 1 α (Ero1 α) and protein disulfide isomerase (PDI) (Wang *et al*, 2015; Fass & Thorpe, 2018). Ero1 α utilizes oxygen as the final electron acceptor for *de novo* disulfide bond formation and transfers disulfides to PDI, which directly catalyzes disulfide formation in reduced substrates (Mezghrani *et al*, 2001; Tu & Weissman, 2002; Sevier & Kaiser, 2008). Ero1 α is upregulated under hypoxic conditions (May *et al*, 2005), highly expressed in many cancers (Battle *et al*, 2013;

1 National Laboratory of Biomacromolecules, CAS Center for Excellence in Biomacromolecules, Institute of Biophysics, Chinese Academy of Sciences, Beijing, China

2 College of Life Sciences, University of Chinese Academy of Sciences, Beijing, China

3 The State Key Laboratory of Protein and Plant Gene Research, School of Life Sciences, Peking University, Beijing, China

4 Academy for Advanced Interdisciplinary Studies, Peking-Tsinghua Center for Life Sciences, Peking University, Beijing, China

5 Laboratory of Proteomics, Institute of Biophysics, Chinese Academy of Sciences, Beijing, China

*Corresponding author. Tel: +86 10 64888501; E-mail: wanglei@moon.ibp.ac.cn

Kukita *et al*, 2015), and involved in calcium flux and cell apoptosis (Li *et al*, 2009; Chin *et al*, 2011).

The byproduct of Ero1 α oxidase activity is hydrogen peroxide (H₂O₂) (Gross *et al*, 2006; Wang *et al*, 2009), which is estimated to account for up to 25% of the cellular reactive oxygen species (ROS) produced during protein synthesis (Tu & Weissman, 2004). Therefore, Ero1 α oxidase activity must be tightly controlled to prevent excess ROS accumulation in resting states and it needs to be activated promptly once robust oxidative protein folding capacity is required. The activity of Ero1 α is feedback regulated by PDI and its homologues to maintain redox balance in the ER (Sevier *et al*, 2007; Kim *et al*, 2012; Zhang *et al*, 2014). Excessive reduction of PDI in the ER induces Ero1 α to undergo regulatory disulfides breakage. Conversely, if the ER is excessively oxidized, the regulatory disulfides will be formed by oxidized PDI to suppress Ero1 α activity (Wang *et al*, 2015; Delaunay-Moisan *et al*, 2017). Besides this “regulatory disulfide switch”, whether any other post-translational modification can regulate Ero1 α activity remains unclear.

Here, we report that Fam20C interacts with a wide range of proteins localized within the secretory pathway and that its deletion disrupts the ER redox poise. We further show that Fam20C phosphorylates Ero1 α at Ser145 in the Golgi apparatus and that ERp44/KDEL receptor (KDELr) mediates the retrograde transport of phosphorylated Ero1 α to the ER. Importantly, phosphorylated Ero1 α displays enhanced oxidase activity and promotes oxidative protein folding. Phosphorylation of Ero1 α at Ser145 by Fam20C is critical for maintaining ER redox homeostasis, and it is induced under hypoxia, reductive stress, and physiological conditions with increased secretory demands such as mammalian lactation. Our study expands Fam20C’s biological roles in the ER lumen and establishes the first link between secretory protein phosphorylation and oxidative protein folding.

Results

Fam20C kinase activity is linked to ER redox homeostasis

To explore the role of secretory kinase Fam20C in the lumen of the secretory pathway, we first identified the Fam20C interactome by co-immunoprecipitation and mass spectrum (MS) analysis (Fig 1A). We identified a total of 349 proteins localized in the ER and Golgi apparatus that specifically interact with Fam20C (Fig 1B), involved in protein processing in the ER, N-glycan biosynthesis, fatty acid metabolism etc., as analyzed by DAVID Gene Ontology (Fig 1C). Notably, enzymes responsible for oxidative protein folding were enriched in the Fam20C interactome, including PDI family proteins (PDI, ERp57, P5, ERp44, and TMX3) and the ER sulfhydryl oxidase Ero1 α (Dataset EV1). Since ER lumen is the compartment for secretory protein folding and its oxidizing environment is critical for protein disulfide formation, we further studied whether Fam20C could affect ER redox homeostasis.

Using the CRISPR/Cas9 technology, we obtained two clones of *FAM20C* knockout (KO) HeLa cells, which harbor frameshift mutations resulting in premature stop codons (Fig EV1A). As a glycosylated protein, Fam20C was detected in Concanavalin A (ConA) precipitates from the conditioned medium of unedited HeLa cells but not of the *FAM20C* KO cells, by immunoblotting with a

polyclonal antibody against the C-terminal peptide of human Fam20C (Fig EV1B). The depletion of *FAM20C* showed little effect on thapsigargin (Tg)-induced unfolded protein response (UPR) signaling, suggesting that *FAM20C* KO does not trigger broad ER stress (Fig EV1C).

To monitor the ER redox, we made a superfolded ER-localized redox-sensitive green fluorescent protein (superfolded-roGFP-iE_{ER}) referring to previous studies (Birk *et al*, 2013; Hoseki *et al*, 2016). The ratio of fluorescence intensity at 390/465 nm excitation of the superfolded-roGFP-iE_{ER} increased under oxidizing conditions and decreased under reducing conditions (Fig EV2). Interestingly, we observed a more reduced ER in the two clones of *FAM20C* KO cells (Fig 1D). Replenishment with Fam20C wild-type (WT) reverted the ER to a state of oxidation, but the catalytically inactive Fam20C D478A (DA) did not (Fig 1E). Among all the ER oxidoreductases identified in the Fam20C interactome, Ero1 α is the pivotal oxidase catalyzing *de novo* disulfide formation, which uses molecular oxygen to oxidize PDI and downstream substrates (Fig 1F). We therefore focused on the interaction between Fam20C and Ero1 α . As shown in Fig 1G, endogenous Ero1 α was indeed immunoprecipitated with Fam20C. Taken together, these results suggest that the kinase activity of Fam20C is linked to the regulation of ER redox homeostasis.

Ero1 α is phosphorylated at Ser145

To determine whether Ero1 α is a phosphoprotein and to identify putative phosphorylation sites, HA-tagged human Ero1 α was expressed in HeLa cells and purified by HA immunoprecipitation (Fig EV3A). Purified Ero1 α was digested with trypsin and subjected to liquid chromatography (LC)-MS/MS. MS analysis yielded 95.7% sequence coverage and identified a single phosphopeptide ¹³⁷LGAVDESLpSEETQK¹⁵⁰ (Fig 2A and B). Especially, the phosphate group-containing y₆⁺ ion was captured in the MS/MS spectrum (Fig 2A), strongly indicating that Ser145 is a genuine phosphorylation site in Ero1 α . Ser145 is C-terminal to the outer active site-containing flexible loop (Fig 2C) and highly conserved in higher eukaryotes (Fig 2D). Subsequently, we generated an anti-phosphorylated Ero1 α (p-Ero1 α) antibody specifically recognizing phosphorylated Ser145 of Ero1 α (Fig EV3B) to facilitate the study of Ser145 phosphorylation. We could clearly detect p-Ero1 α in HA precipitates from cell extracts and in ConA precipitates from the conditioned medium of HeLa cells overexpressing Ero1 α WT, but not Ero1 α S145A mutant (Fig 2E). Moreover, when treated with λ -protein phosphatase, p-Ero1 α signals in the conditioned medium remarkably diminished (Fig 2F). Thus, phosphorylation of Ero1 α in cells occurs at Ser145.

Ero1 α phosphorylation is catalyzed by Fam20C

Ero1 α Ser145 lies within the Fam20C S-x-E/pS recognition motif, and we next investigated whether Fam20C phosphorylates Ero1 α . An *in vitro* kinase assay showed that purified Fam20C protein phosphorylated recombinant Ero1 α in a time-dependent manner, as confirmed by the slowly migrating bands and by p-Ero1 α blotting. In contrast, the inactive Fam20C DA mutant failed to incorporate phosphate into Ero1 α (Fig 3A). In HeLa and HepG2 cells, overexpressed Fam20C effectively catalyzed phosphorylation of endogenous Ero1 α

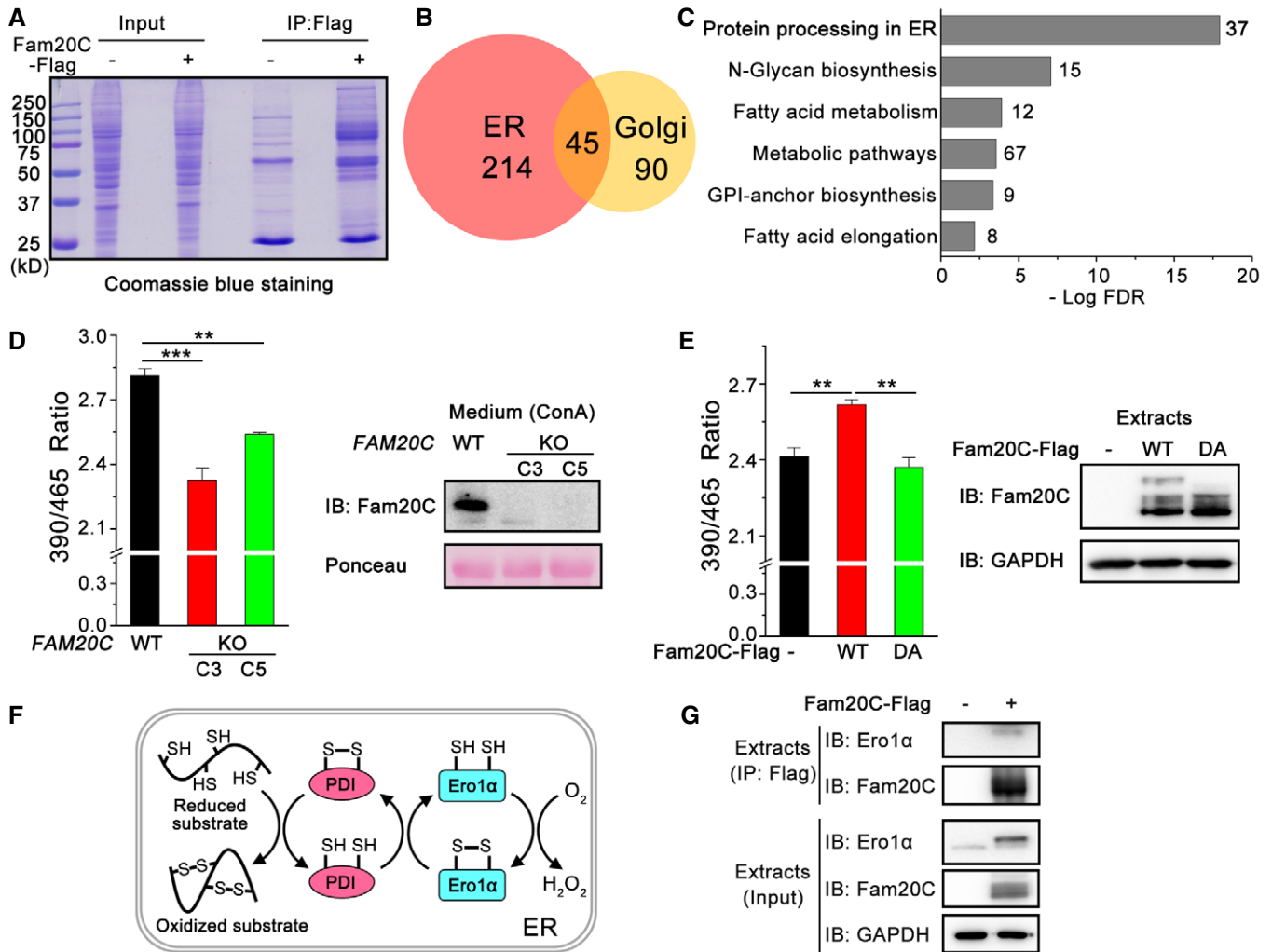


Figure 1. FAM20C KO triggers a reduced ER.

A Coomassie Blue Staining of Flag immunoprecipitates from HeLa cells expressing Fam20C-Flag for MS analysis.
 B Venn diagram of the 349 proteins interacting with Fam20C identified in the ER and Golgi apparatus based on DAVID GO term analysis.
 C KEGG pathway mapping of the most enriched biological processes in the Fam20C interactome in the ER and Golgi. The graph represents the top six statistically significant enriched gene clusters ordered by FDR (false discovery rate), with the number of genes in each cluster indicated beside the bars.
 D (Left) Fluorescence intensities of superfolded-roGFP-iE_{ER} in wild-type (WT) and two clones (C3 and C5) of FAM20C KO HeLa cells at 525 nm were measured with excitation at 390 and 465 nm. The fluorescence ratio at 390/465 nm excitation was calculated. Data are shown as mean \pm SEM from five (WT and C3) or three (C5) independent experiments performed in six technical replicates. ****P** < 0.01, *****P** < 0.001 (one-way ANOVA, the *post hoc* Tukey's HSD test). (Right) Protein immunoblotting of Concanavalin A (ConA) precipitates from the culture medium of WT and FAM20C KO HeLa cells. Ponceau staining is shown as a loading control.
 E (Left) Fluorescence intensities of superfolded-roGFP-iE_{ER} in FAM20C KO HeLa cells expressing Fam20C WT or its inactive mutant D478A (DA) were measured as in (D). Data are shown as mean \pm SEM from four independent experiments performed in six technical replicates. ****P** < 0.01 (one-way ANOVA, the *post hoc* Tukey's HSD test). (Right) Protein immunoblotting of FAM20C KO HeLa cells expressing Fam20C WT or DA.
 F Schematic representation of the pivotal pathway constituted by Ero1 α and PDI for oxidative protein folding in the mammalian ER.
 G Co-immunoprecipitation of endogenous Ero1 α and Flag-tagged Fam20C in HeLa cells.

Source data are available online for this figure.

(Fig 3B). When we knocked Fam20C out or down in the HeLa cells, Ero1 α was no longer phosphorylated (Figs 3C and EV3C). Moreover, by either immunoblotting (Fig 3D) or immunofluorescence (Fig 3E), we observed p-Ero1 α in cells co-expressing Ero1 α and Fam20C WT but not Fam20C DA. Immunofluorescence analysis also showed that p-Ero1 α and Fam20C displayed subcellular colocalization (Fig 3F), and co-immunoprecipitation experiments supported the finding that p-Ero1 α and Fam20C interacted physically

(Fig EV3D). Convincingly, Fam20C is the *bona fide* kinase catalyzing Ero1 α Ser145 phosphorylation.

Ero1 α is phosphorylated by Fam20C in the Golgi and retained in the ER by ERp44

Fam20C-catalyzed protein phosphorylation is believed to occur in the Golgi lumen or the extracellular space (Tagliabracci *et al*, 2013).

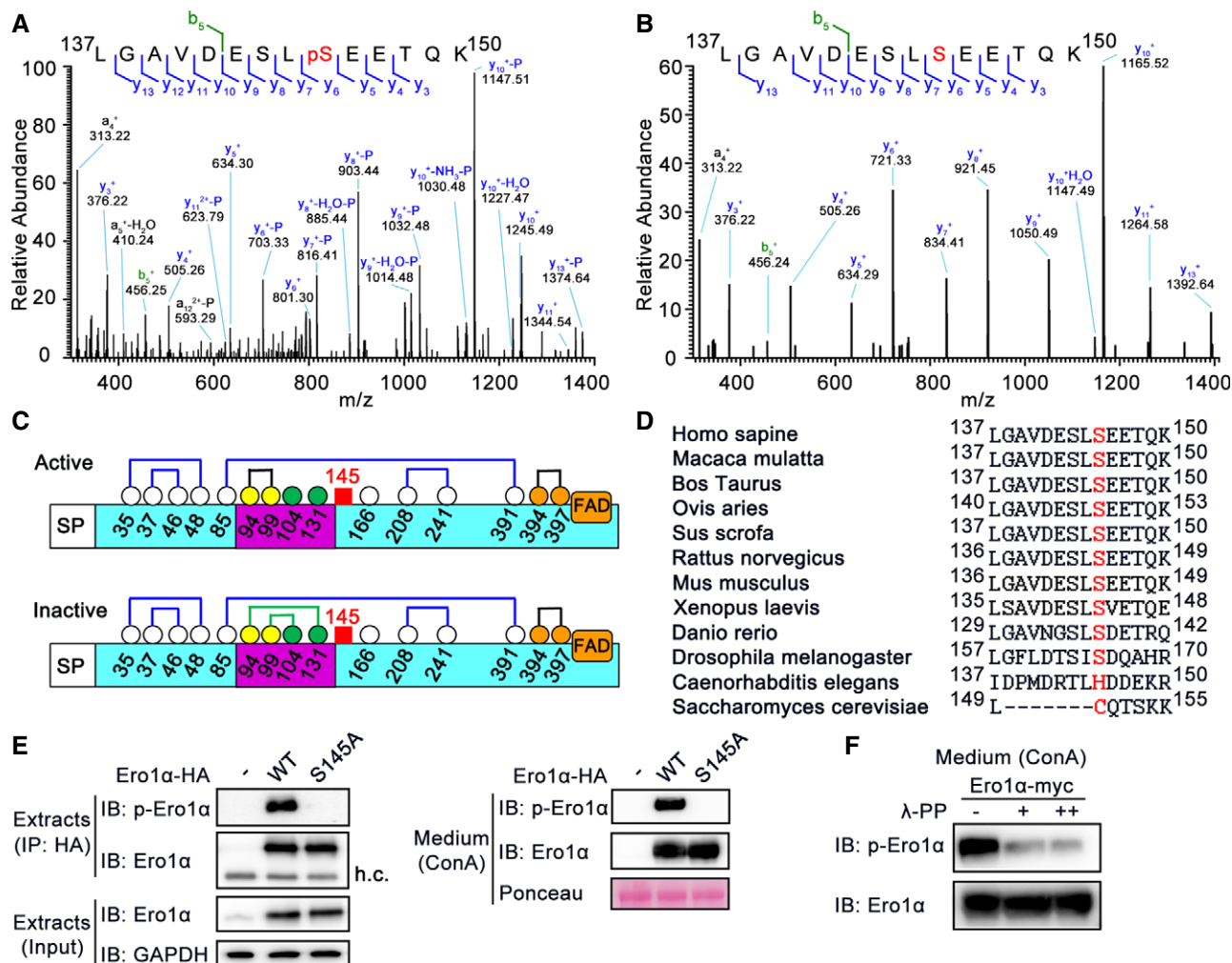


Figure 2. Ero1 α can be phosphorylated at Ser145.

A, B Representative MS/MS fragmentation spectra of tryptic phosphorylated (A) and non-phosphorylated (B) peptides (Ero1 α Leu137–Lys150) depicting Ero1 α Ser145 phosphorylation enriched from Ero1 α -overexpressed HeLa cells.

C Schematic representation of human Ero1 α active and inactive forms depicting signal peptide (SP), flexible loop (lilac), and cofactor FAD. The cysteines are shown as circles of white, yellow (outer active site), orange (inner active site), or green (regulatory cysteines) with amino acid numbering, disulfides as lines of blue (structural), black (active site), or green (regulatory), and Ser145 as a red square.

D Amino acid sequence alignments of Ero1 α homologues in several species by BLAST. Residue positions are indicated by numbers counted from the N-terminus. Human Ero1 α Ser145 and its counterparts are shown in red.

E Detection of phosphorylated Ero1 α (p-Ero1 α) in HeLa cells overexpressing HA-tagged Ero1 α WT or S145A (Left), or in ConA precipitates from the conditioned medium (Right). h.c.: heavy chain.

F Protein immunoblotting of ConA precipitates treated with λ -phosphatase (λ -PP) from the conditioned medium of HeLa cells overexpressing Ero1 α .

Source data are available online for this figure.

Ero1 α is predominantly located in the ER lumen at basal level and can also be secreted into the extracellular space when its expression is greatly elevated (Cabibbo *et al*, 2000; Anelli *et al*, 2003). Accordingly, we detected p-Ero1 α in both cell extracts and culture medium (Fig 2E). Thus, a key question is where Ero1 α phosphorylation occurs. To address this, we compared HeLa cells co-expressing Ero1 α and Fam20C with co-cultured cells expressing Ero1 α and Fam20C individually. If Ero1 α can be phosphorylated in the extracellular space, a p-Ero1 α signal should be observable in the culture medium of the latter group. However, in both the cell extracts and conditioned medium, we detected p-Ero1 α only in cells

co-expressing Ero1 α and Fam20C, not in the co-cultured group. This strongly suggests that Fam20C phosphorylates the secreted Ero1 α within cells (Fig 4A).

In cells, we observed p-Ero1 α in both the ER and the Golgi lumen by immunofluorescence, using PDI and GM130 as respective markers (Fig 4B), and also by subcellular fractionation (Fig EV4A). To learn whether Ero1 α phosphorylation catalyzed by Fam20C occurs in the ER or Golgi apparatus, we engineered a KDEL retrieval sequence to the C-terminus of Ero1 α , which can be sequestered by cis-Golgi-anchored KDEL. This engineering would enhance ER localization of Ero1 α and decrease the amount that traverses the late

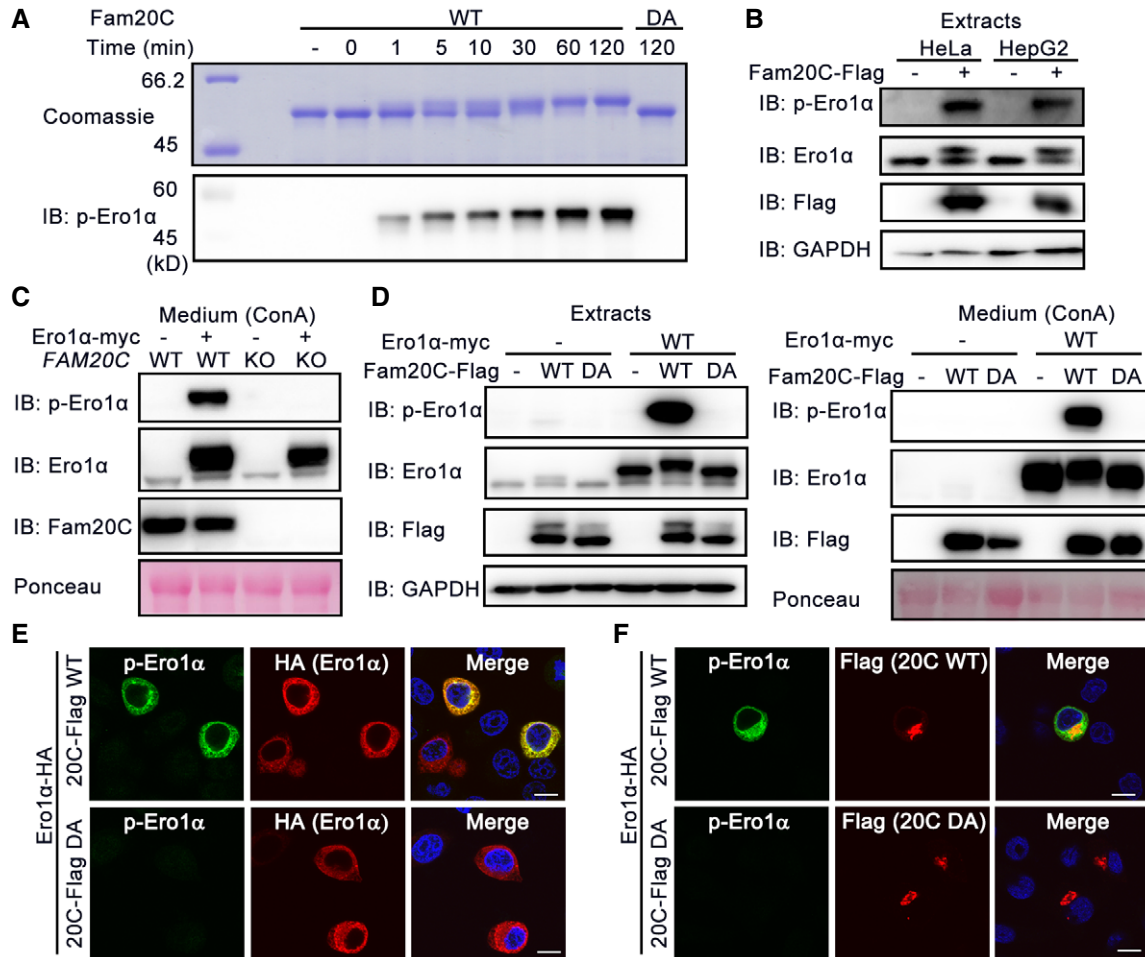


Figure 3. Ero1 α phosphorylation is catalyzed by Fam20C.

- A Time-dependent incorporation of phosphate group into Ero1 α catalyzed by recombinant Fam20C WT or DA mutant. Reaction products were analyzed by Coomassie Blue staining and p-Ero1 α immunoblotting.
- B Detection of endogenous p-Ero1 α in HeLa and HepG2 cells overexpressing Fam20C.
- C Protein immunoblotting of ConA precipitates from the conditioned medium of WT or FAM20C KO HeLa cells transfected with or without Ero1 α -myc.
- D Protein immunoblotting of cell extracts (*Left*) and ConA precipitates from the conditioned medium (*Right*) of HeLa cells co-expressing Ero1 α -myc and/or Fam20C-Flag WT or DA.
- E, F Immunofluorescence analysis of p-Ero1 α in HepG2 cells co-expressing Ero1 α -HA and Fam20C-Flag WT or DA. Scale bars = 10 μ m.

Source data are available online for this figure.

secretory pathway. As expected, Ero1 α -KDEL was largely retained in cells compared to WT Ero1 α (Fig 4C). Strikingly, Ero1 α -KDEL was less phosphorylated in cells, indicating that it is in the Golgi cisternae where Fam20C phosphorylates Ero1 α and that p-Ero1 α is then retrograde-transported to the ER (Fig 4C). It is known that the ER retention of Ero1 α is accomplished by ERp44, a PDI family chaperone ensuring ER retrieval via KDEL in the early secretory pathway (Anelli *et al*, 2003; Wang *et al*, 2008; Vavassori *et al*, 2013). We propose that relocation of p-Ero1 α to the ER is also achieved by ERp44. Indeed, p-Ero1 α could be co-immunoprecipitated with ERp44 and the secretion of p-Ero1 α dramatically decreased with ERp44 overexpression (Fig 4D), though ERp44 bound to Ero1 α WT, S145A and S145E mutants and retained them within the ER with similar affinities (Fig EV4B and C). When we knocked ERp44 down using siRNA in HeLa cells, a higher amount of p-Ero1 α was released to the

culture medium (Fig 4E). Taken together, these results indicate that Ero1 α phosphorylation occurs in the Golgi, catalyzed by Fam20C, and that ERp44/KDEL achieves the retention of p-Ero1 α in the ER.

p-Ero1 α displays higher sulfhydryl oxidase activity

Protein phosphorylation is a common way to induce changes in protein conformation and activity. Based on its crystal structure, Ero1 α Ser145 is located at the C-terminus of the outer active site (Cys94-Cys99)-containing flexible loop, the movement of which is critical for shuttling electrons from PDI to Ero1 α inner active site (Cys394-Cys397) (Fig 5A). Since Ero1 α uses oxygen to catalyze *de novo* disulfide bond formation in the electron transfer pathways (Fig 5B), we monitored the oxygen consumption rate via an oxygen electrode to study the effect of phosphorylation on Ero1 α activity.

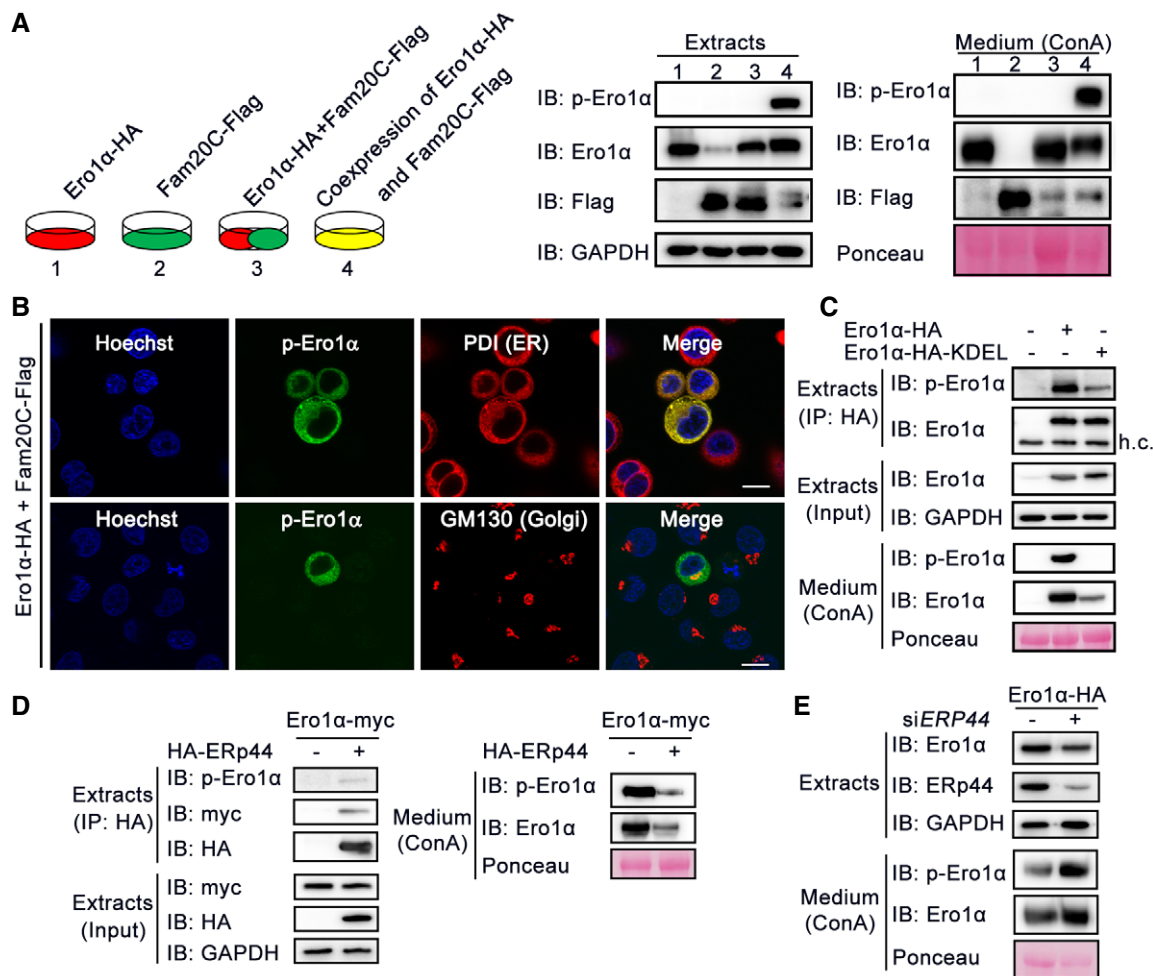


Figure 4. Ero1 α is phosphorylated by Fam20C in the Golgi and retained in the ER by ERp44.

- A Protein immunoblotting of cell extracts and ConA precipitates from the conditioned medium of HeLa cells transfected with Ero1 α (1) or Fam20C (2) alone, or co-transfected with Ero1 α and Fam20C (4), or co-cultured cells expressing Ero1 α and Fam20C separately (3).
- B Immunofluorescence analysis showing the subcellular localization of p-Ero1 α in HepG2 cells co-expressing Ero1 α and Fam20C. PDI and GM130 were used as ER and Golgi markers, respectively. Scale bars = 10 μ m.
- C Protein immunoblotting of cell extracts and ConA precipitates from the conditioned medium of HeLa cells overexpressing Ero1 α -HA or Ero1 α -HA-KDEL.
- D Co-immunoprecipitation of ERp44 and Ero1 α /p-Ero1 α (Left) and protein immunoblotting of ConA precipitates from the conditioned medium (Right) in HeLa cells expressing Ero1 α -myc alone or with HA-ERp44.
- E Protein immunoblotting of cell extracts and ConA precipitates from the conditioned medium of HeLa cells transfected with Ero1 α -HA and scramble siRNA or siRNA targeting *ERP44*.

Source data are available online for this figure.

The Ero1 α phosphorylation mimic S145E displayed twofold higher oxidase activity than that of Ero1 α WT in the presence of either the small molecule reducing agent dithiothreitol (DTT) (Fig 5C) or the physiological substrate PDI reduced by glutathione (GSH) (Fig 5D). Mutation of the two non-catalytic cysteines, Cys104 and Cys131, disrupts the regulatory disulfides in Ero1 α and results in a constitutively active oxidase (Appenzeller-Herzog *et al*, 2008; Baker *et al*, 2008). Notably, Ero1 α C104A/C131A/S145E, a hyperactive Ero1 α phosphorylation mimic, showed further increased activity (Fig 5C and D), suggesting that Ser145 phosphorylation is a novel activity controller independent of the known “regulatory disulfide switch” in Ero1 α . To further confirm the regulatory role of Ser145 phosphorylation, we prepared genuine phosphorylated Ero1 α using an *in vitro*

kinase assay. Consistent with the results obtained from the phosphorylation mimics, both p-Ero1 α WT and p-Ero1 α C104A/C131A exhibited twice the activity of Ero1 α WT and C104A/C131A (Fig 5E and F).

Acceleration of PDI oxidation caused by Ser145 phosphorylation still depended on the presence of the Ero1 α outer active site (Fig EV5A), implying that phosphorylation does not alter the electron transfer pathway. Moreover, the steady redox state (Fig EV5B) and reduced PDI-mediated activation (Fig EV5C) of p-Ero1 α mimics showed no difference from those of Ero1 α , suggesting that phosphorylation does not affect allosteric activation of Ero1 α . As Ser145 is located between the flexible loop region and an adjacent α -helix (Fig 5A), we investigated whether its phosphorylation results in a conformational change in Ero1 α . Although the overall secondary

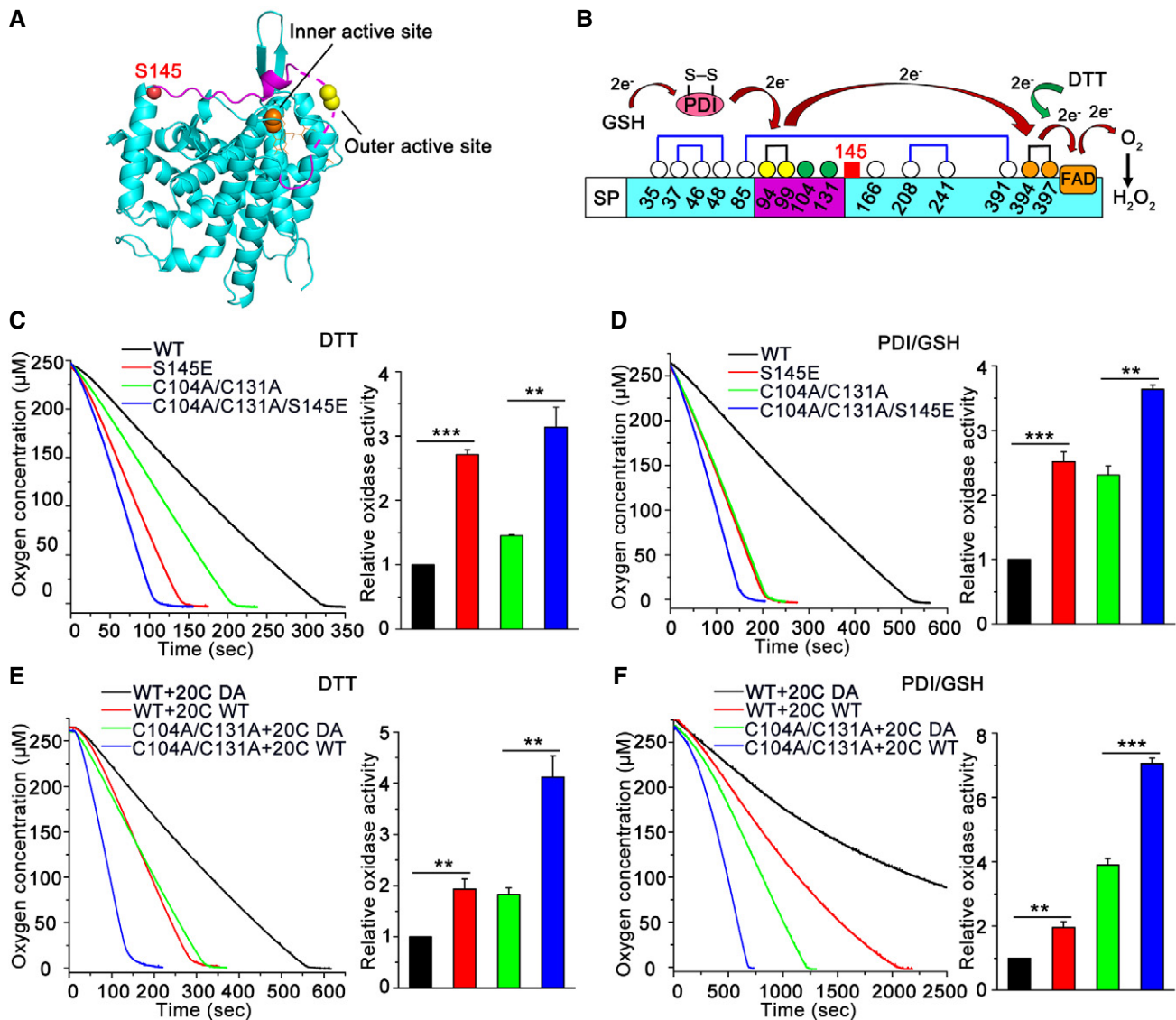


Figure 5. Phosphorylation of Ero1 α increases its sulfhydryl oxidase activity *in vitro*.

A Ribbon representation of the active form of human Ero1 α structure (PDB: 3AHQ). Outer active site (yellow ball), inner active site (orange ball), cofactor FAD (orange stick), and Ser145 (red ball) are indicated. The outer active site-containing loop is shown in lilac and the missing region by the dashed line.

B Schematic representation of the electron transfer pathway between the active sites of Ero1 α and its physiological substrate PDI/GSH or small molecule reducing agent DTT.

C–F Oxygen consumption catalyzed by Ero1 α phosphorylation mimics (C, D) or Fam20C-treated Ero1 α (E, F), on a background of Ero1 α WT or hyperactive C104A/C131A, was monitored in the presence of DTT (C, E) or PDI and GSH (D, F). The relative oxidase activity of Ero1 α was calculated from the slope of the linear phase of oxygen decrease. Data are shown as mean \pm SEM from three independent experiments. ** $P < 0.01$, *** $P < 0.001$ (two-tailed, Student's *t*-test).

structure of Ero1 α S145E was similar to that of Ero1 α WT as shown by the circular dichroism spectrum (Fig EV5D), we observed an increase in intrinsic tryptophan fluorescence in Ero1 α S145E (Fig EV5E), implying that microenvironment changes occur around the aromatic residues. We also noticed from the crystal structure of Ero1 α that there is a hydrogen bond between the O atom of the Ser145 hydroxyl group and the N atom of the Thr148 main chain, and this hydrogen bond would be disfavored due to the presence of a phosphate group on the side chain of Ser145 (Fig EV5F). The conformational change induced by phosphorylation may increase

the flexibility of the outer active site-containing flexible loop and contribute to the higher oxidase activity of p-Ero1 α .

Phosphorylation of Ero1 α Ser145 plays a critical role in ER redox homeostasis

To investigate whether phosphorylation of Ero1 α Ser145 by Fam20C is linked to ER redox regulation, we first generated *ERO1A* KO HeLa cells by means of CRISPR/Cas9 genome editing (Fig EV6). Using the superfolded-roGFP-iE_{ER} probe, we observed a dramatically reduced

ER redox environment in the two clones of *ERO1A* KO cells (Fig 6A), underlining the importance of Ero1 α in maintaining ER redox homeostasis. The redox state in the ER was partially recovered by the replenishment of Ero1 α WT and further restored by Ero1 α S145E, indicating that p-Ero1 α is also more active in cells (Fig 6B). Importantly, the expression of Fam20C in *ERO1A* KO cells transfected with Ero1 α WT resulted in the phosphorylation of the majority of Ero1 α and generated a more oxidized ER (Fig 6C). However, the expression of Fam20C in *ERO1A* KO cells or in Ero1 α S145A-transfected *ERO1A* KO cells exhibited little effect on the ER redox state (Fig 6C). Therefore, we conclude that Fam20C participates in ER redox regulation through the phosphorylation of Ero1 α Ser145.

Phosphorylation of Ero1 α promotes oxidative protein folding

We next explored whether Ero1 α phosphorylation promotes oxidative protein folding in cells by monitoring the folding of immunoglobulin J-chain, a specific substrate of Ero1 α (Mezghrani et al, 2001). As shown in Fig 7A, when HeLa transfectants expressing Myc-tagged

J-chain (JcM) were briefly exposed to DTT, most JcM migrated as reduced monomers. Upon removal of DTT, those monomers progressively disappeared, and in turn, oxidized monomers and dimers emerged. Compared to cells co-expressing an inactive Ero1 α mutant C99A/C104A, oxidized JcM monomers and dimers formed more rapidly during the chase phase in cells co-expressing Ero1 α WT, and more high-molecular-weight (HMW) species were observed. In accordance with the *in vitro* results, the Ero1 α phosphorylation mimic S145E significantly accelerated the J-chain folding process in cells compared to Ero1 α WT, as quantified by the disappearance of reduced monomers (Fig 7B). Furthermore, the transition of reduced JcM into oxidized species was also faster in HeLa cells overexpressing Fam20C WT than in cells expressing Fam20C DA (Fig 7C and D), probably due to the elevated level of endogenous p-Ero1 α . In contrast, in the *ERO1A* KO cells, the re-oxidation of JcM was completely repressed, and ectopic expression of either Fam20C WT or DA had little effect on JcM re-oxidation (Fig 7C and D). Altogether, these results suggest that phosphorylation of Ero1 α Ser145 by Fam20C does promote oxidative protein folding in cells.

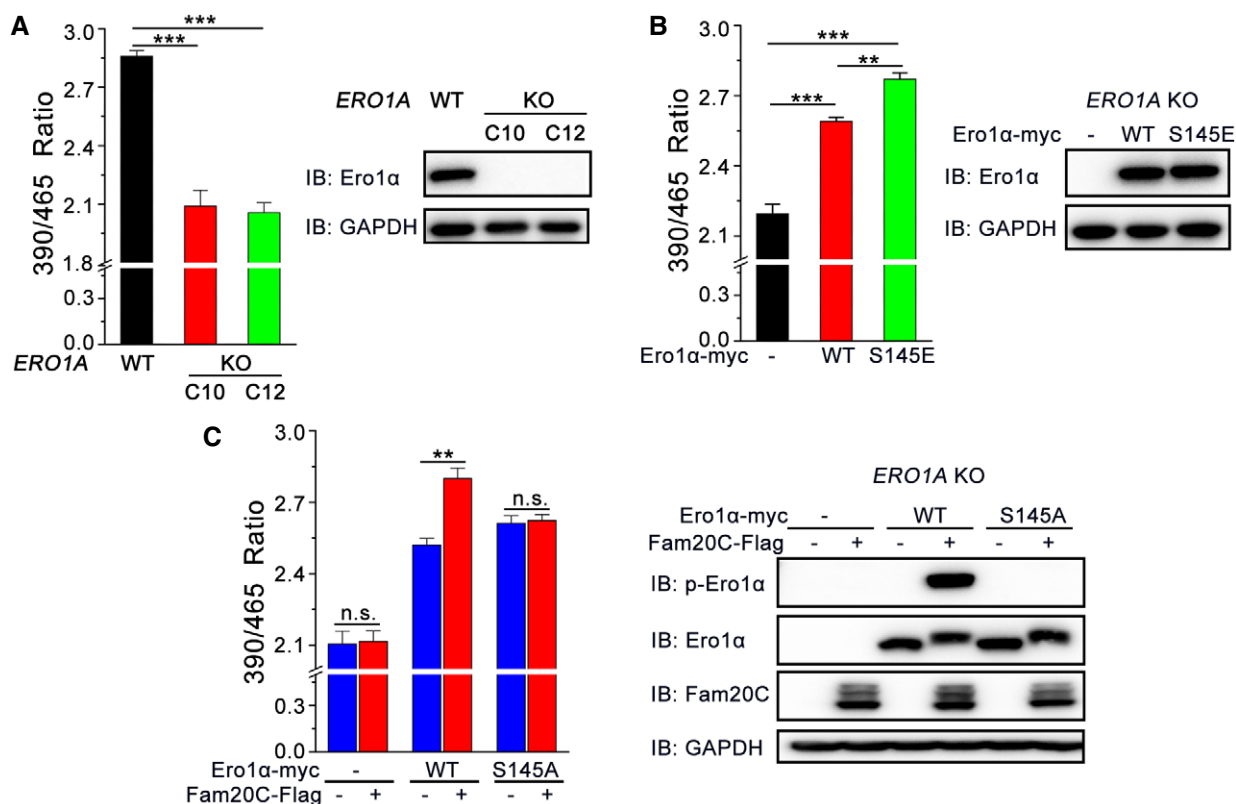


Figure 6. Phosphorylation of Ero1 α Ser145 plays a critical role in ER redox homeostasis.

A (Left) The fluorescence intensities of superfolded-roGFP-iE_{ER} in WT and two clones (C10 and C12) of *ERO1A* KO HeLa cells were measured as in Fig 1D. (Right) Aliquots of cells in the left panel were analyzed by immunoblotting.

B (Left) The fluorescence intensities of superfolded-roGFP-iE_{ER} in *ERO1A* KO HeLa cells expressing Ero1 α -myc WT or S145E were measured as in Fig 1D. (Right) Aliquots of cells in the left panel were analyzed by immunoblotting.

C (Left) The fluorescence intensities of superfolded-roGFP-iE_{ER} in *ERO1A* KO HeLa cells expressing Ero1 α -myc WT or S145A and/or Fam20C-Flag were measured as in Fig 1D. (Right) Aliquots of cells in the left panel were analyzed by immunoblotting.

Data information: All of the data are shown as mean \pm SEM from four independent experiments performed in six technical replicates. ** P < 0.01, *** P < 0.001 (one-way ANOVA, the *post hoc* Tukey's HSD test).

Source data are available online for this figure.

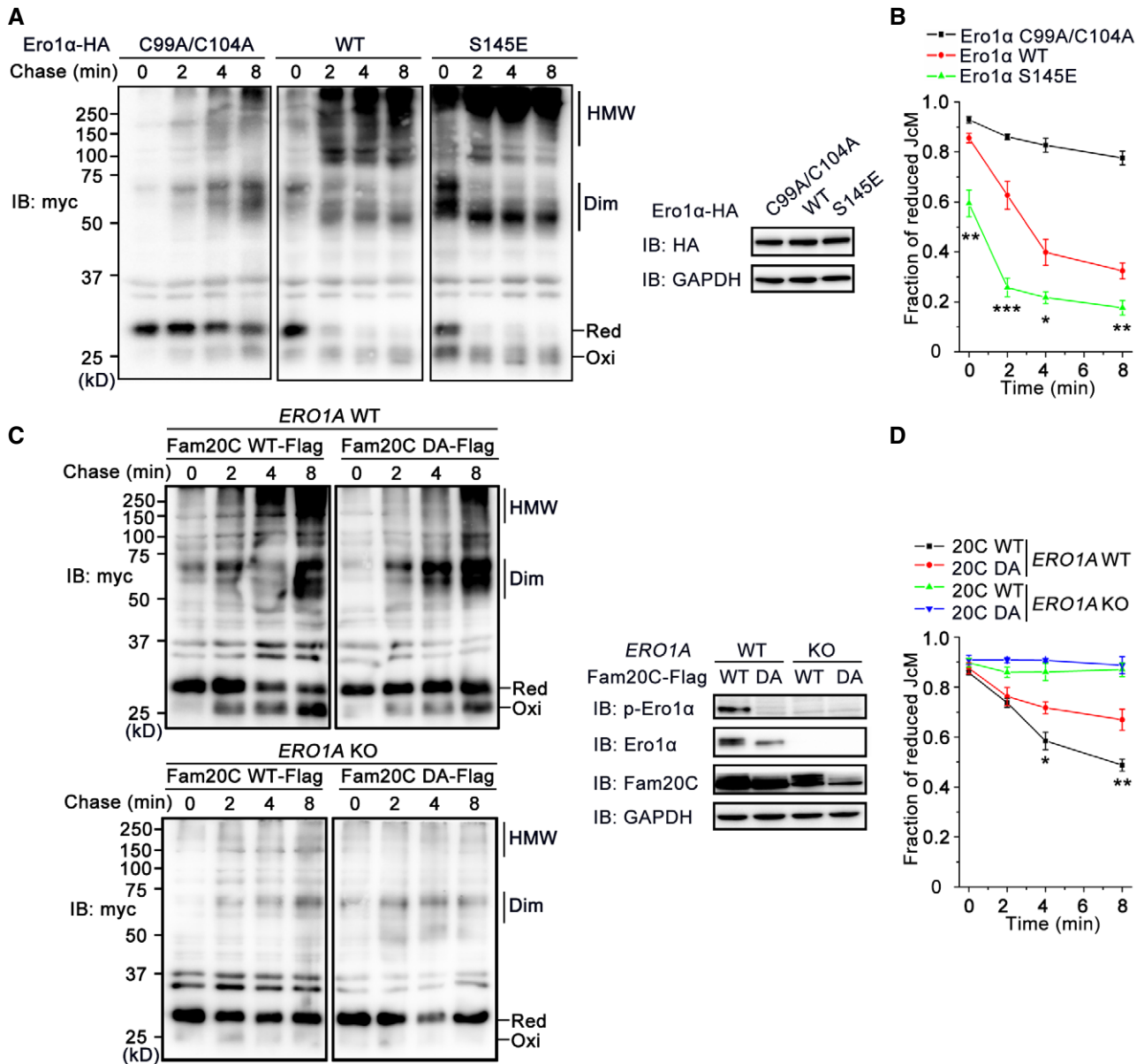


Figure 7. Phosphorylation of Ero1 α promotes oxidative protein folding in cells.

A (Left) HeLa transfectants expressing myc-tagged JcM with Ero1 α -HA C99A/C104A, WT, or S145E were pulsed with DTT, washed, and chased at indicated time points by non-reducing myc blotting. The mobility of reduced JcM monomers (Red), oxidized monomers (Oxi), homodimers (Dim), and high-molecular-weight (HMW) species is indicated. (Right) Aliquots from cell lysates in the left panel were resolved in reducing conditions and analyzed by immunoblotting.

B The fraction of reduced JcM (Red/[Red + Oxi]) in (A) was quantified by densitometry. Data are shown as mean \pm SEM from five independent experiments. * P < 0.05, ** P < 0.01, *** P < 0.001, between Ero1 α WT and S145E (two-tailed Student's t -test).

C (Left) JcM re-oxidation in WT and ERO1A KO HeLa cells overexpressing Fam20C-Flag WT or DA was monitored as in (A). (Right) Aliquots from cell lysates in the left were resolved in reducing conditions and analyzed by immunoblotting.

D The fraction of reduced JcM in (C) was quantified by densitometry. Data are shown as mean \pm SEM from four independent experiments. * P < 0.05, ** P < 0.01, between Fam20C-Flag WT and DA in WT HeLa cells (two-tailed Student's t -test).

Source data are available online for this figure.

Phosphorylation of Ero1 α is induced during mammalian lactation, hypoxia, and reductive stress

To determine whether Fam20C can phosphorylate Ero1 α in physiological processes, we first focused on mammalian lactation, during

which abundant secretory proteins are produced. Figure 8A shows that mRNA levels of FAM20C and its activator FAM20A, which encodes a pseudokinase that forms a functional complex with Fam20C to enhance secretory protein phosphorylation, were dramatically elevated in mammary glands of lactating mice

compared to those of virgin mice, consistent with the previous report (Cui *et al*, 2015). Interestingly, *ERO1A* and *PDIA1* mRNAs were also greatly upregulated in lactating mammary glands. Consistent with their mRNA levels, Ero1 α and Fam20C proteins were more abundant in lactating mouse mammary glands (Fig 8B). Notably, we could clearly detect a much stronger p-Ero1 α signal and a significantly higher ratio of p-Ero1 α /Ero1 α in the mammary glands of lactating mice than those of virgin mice (Fig 8B and C). Altogether, these results demonstrate that Fam20C phosphorylates Ero1 α in the mammary glands of lactating animals.

It has been known that hypoxic induction of Ero1 α is the key adaptive response to improve protein secretion under hypoxia (May *et al*, 2005). Notably, when Fam20C-expressing HeLa cells were cultured in a hypoxic chamber with 0.1% oxygen concentration, phosphorylation of Ero1 α was dramatically induced along with an increase in total Ero1 α and hypoxia-inducible factor 1 (HIF-1 α) (Fig 8D). We also investigated whether phosphorylation of Ero1 α could be induced during ER stress or reductive stress by pharmacological modulation. When Fam20C-expressing cells were treated with known ER stress inducers, including Tg (an inhibitor of sarco/endoplasmic reticulum Ca²⁺-ATPase (SERCA) calcium pump), tunicamycin (Tm; an inhibitor of protein glycosylation), and Brefeldin A (BFA; an inhibitor of ER-Golgi traffic), both p-Ero1 α and total Ero1 α level were unchanged up to 6 h, though IRE1 α and PERK UPR branches were activated (Fig 8E). Interestingly, when cells were treated with 200 μ M DTT, a concentration sufficient to reduce protein disulfides but not trigger UPR, p-Ero1 α was rapidly and strongly induced whereas total Ero1 α protein level did not change (Fig 8E and F). These results suggest that Fam20C-catalyzed phosphorylation of Ero1 α occurs as a post-translational regulatory mechanism to counteract cellular reductive stress.

Discussion

In this study, we report Fam20C, the Golgi-localized secretory kinase, has a previously unidentified function of fine-tuning ER redox homeostasis and oxidative protein folding. Ero1 α , an ER sulfhydryl oxidase, can be transported to the Golgi apparatus and effectively phosphorylated by Fam20C at Ser145. Phosphorylation of Ero1 α largely enhances its oxidase activity. Similar to non-phosphorylated Ero1 α , phosphorylated Ero1 α is relocated to the ER lumen, also mediated by the ERp44/KDEL system, to promote disulfide bond formation and maintain ER redox homeostasis (Fig 8G). This model also provides an answer to the long-unsolved question of why Ero1 α functions in the ER but does not contain an ER retention motif. Indeed, engineered Ero1 α -KDEL protein is more resistant to phosphorylation by Fam20C (Fig 4C). Although it is possible that Fam20C is active during its transit route across the ER, we propose that a rather unique milieu in the Golgi is appropriate for Fam20C activity. Besides Ero1 α and the recently reported sarcoplasmic reticulum histidine-rich calcium-binding protein (HRC) (Pollak *et al*, 2017), we identify several ER/Golgi-localized enzymes and chaperones that also interact with Fam20C (Fig 1 and Dataset EV1). Future studies are required to determine whether these proteins can be phosphorylated by Fam20C and can therefore participate in certain biological processes.

Professional secretory cells and tissues have extremely high demands for oxidative protein folding in the ER. For example, lactating mammary glands produce milk, which contains a large amount of disulfide-rich proteins (e.g., immunoglobulins, α -lactalbumin, and serum albumin). Indeed, the expression of both Fam20C and Ero1 α is dramatically elevated in lactating mouse mammary glands. Notably, we have detected strong p-Ero1 α signals in the mammary glands of lactating mice, suggesting that Ero1 α phosphorylation by Fam20C plays an important role in lactation. Interestingly, we find that p-Ero1 α is not induced under ER stress caused by calcium depletion or aberrant glycosylation; instead, it is rapidly induced once the protein disulfides in the ER are disrupted by the reducing agent DTT. Since oxygen is the ultimate source of oxidizing power for disulfide formation, it is also reasonable that p-Ero1 α is induced under hypoxic condition to increase the bioavailability of oxygen. Previous studies showed that exposure of cells to reductive stress or hypoxia leads to the relocation of Ero1 α from the early secretory pathway to the late secretory pathway (Gilady *et al*, 2010), which is in line with our conclusion that Ero1 α is phosphorylated by Fam20C in the Golgi. Altogether, our study highlights the importance of phosphorylation of Ero1 α by Fam20C as a novel regulatory mechanism to counteract cellular reductive stress at post-translational level. Whether Ero1 α phosphorylation is also enhanced in other secretory cells, such as plasma cells secreting immunoglobulins and β -cells secreting insulin, and is important for efficient oxidative protein folding in those cells are still open questions.

Ero1 oxidase catalyzes one disulfide bond formation and produces one molecule of H₂O₂ as a byproduct; therefore, its activity should be tightly controlled to prevent excess ROS production (Gross *et al*, 2006; Wang *et al*, 2009, 2011). Ero1 activity can be allosterically controlled by “regulatory disulfides”, which were first studied in yeast (Gross *et al*, 2004; Sevier *et al*, 2007; Vitu *et al*, 2010; Kim *et al*, 2012) and later dissected in mammals (Appenzeller-Herzog *et al*, 2008; Baker *et al*, 2008; Inaba *et al*, 2010; Wang *et al*, 2011; Zhang *et al*, 2014). Interestingly, Ser145 in Ero1 α is highly conserved in multicellular organisms but missing in yeast Ero1p (Fig 2D), and Fam20C homologue is not present in yeast, implying that Ero1p is lack of phosphorylation regulation. Instead, yeast Ero1p harbors Cys150 in the same position, and disruption of the Cys150-Cys295 allosteric disulfide is known to enhance the movement of outer active site-containing loop and increase Ero1p activity (Sevier *et al*, 2007), though physiological reduction in the Cys150-Cys295 disulfide requires extremely reducing condition (Niu *et al*, 2016). The homology between Cys150 in Ero1p and Ser145 in Ero1 α further suggests that modification of Ser145 is likely to cause a similar conformational change and enzymatic enhancement. Besides previous reports on the regulatory disulfides of Ero1 α , our observation that Ero1 α can be phosphor-regulated via Ser145 adds an additional layer to the regulation of Ero1 α activity. These findings suggest that human Ero1 α has undergone extensive evolution to optimize the folding efficiency of large, complicated disulfide-containing secretory proteomes and to simultaneously minimize the risks of overoxidation in the ER. Whether Ero1 α possesses other phosphorylation sites besides Ser145, the manner by which these phosphorylation sites orchestrate to regulate ER redox, and the identity of the protein phosphatase for dephosphorylating Ero1 α remain open questions.

Apart from the introduction of disulfide bonds, Ero1 α has also been reported to regulate ER Ca²⁺ influx and efflux. A fraction of

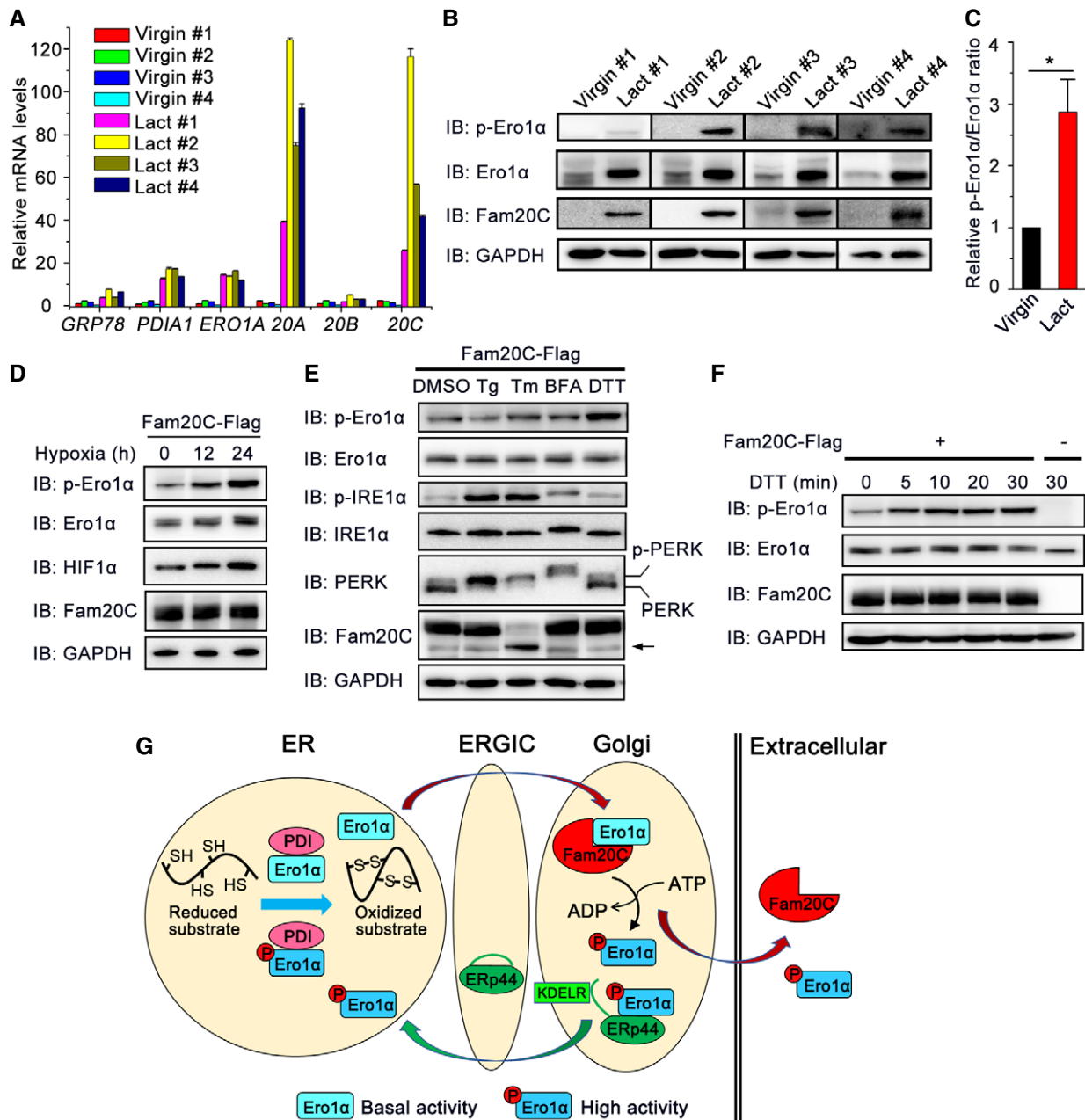


Figure 8. p-Ero1 α is induced during mammalian lactation, hypoxia, and reductive stress.

A mRNA levels of several ER folding catalysts and Fam20 family members in the mouse mammary gland. The mammary glands of four virgin and four lactating (Lact) mice were isolated, and their mRNA levels were determined by RT-qPCR and normalized to the mean value of the virgin group. Data are represented as mean \pm SEM performed in six technical replicates.

B Protein immunoblotting of extracts from the whole mammary glands of virgin and lactating mice.

C Quantification of relative p-Ero1 α /Ero1 α ratio in (B). Data are shown as mean \pm SEM of four groups. * P < 0.05 (two-tailed, Student's t -test).

D Protein immunoblotting of HeLa cells expressing Fam20C-Flag following exposure to hypoxia (0.1% oxygen) for the indicated times.

E Protein immunoblotting of HeLa cells expressing Fam20C-Flag treated with 5 μ M thapsigargin (Tg), 5 μ g/ml tunicamycin (Tm), 5 μ g/ml Brefeldin A (BFA), or 200 μ M DTT for 6 h. The arrow indicates an unglycosylated form of Fam20C.

F Protein immunoblotting of HeLa cells transfected with or without Fam20C-Flag treated with 200 μ M DTT for the indicated times.

G A working model for Fam20C tuning ER redox homeostasis and oxidative protein folding. Ero1 α and PDI catalyze protein disulfide formation in the ER lumen. During mammalian lactation, hypoxia, and reductive stress, non-phosphorylated Ero1 α with basal activity is transported to the Golgi apparatus and phosphorylated by Fam20C at Ser145. Phosphorylated Ero1 α is sequestered by Erp44, a chaperone primarily localized in the ER-Golgi intermediate compartment (ERGIC), and relocated to the ER mediated by KDEL receptor (KDELr). Phosphorylated Ero1 α displays higher oxidase activity to promote disulfide bond formation and maintain ER redox homeostasis.

Source data are available online for this figure.

Ero1 α is localized in mitochondrial-associated ER membranes (Gilady *et al*, 2010; Rammig & Appenzeller-Herzog, 2012). Ero1 α can inhibit SERCA calcium pump activity (Marino *et al*, 2015) and activate inositol 1,4,5-triphosphate receptor 1 (IP₃R1) to induce Ca²⁺ release into the mitochondria and trigger apoptosis (Li *et al*, 2009; Anelli *et al*, 2012), doing both in a redox-dependent manner. Thus, it would be interesting to investigate whether p-Ero1 α with high oxidase activity participates in the regulation of ER calcium homeostasis. Although Ero1 α predominantly localizes and functions in the ER lumen under normal conditions, it can be secreted into the extracellular space at an upregulated level of expression (Cabibbo *et al*, 2000; Anelli *et al*, 2003). However, the role of secreted Ero1 α is largely unknown. In this study, we observe that p-Ero1 α is present in both cell extracts and culture medium (Figs 2E and 3C and D), implying that secreted p-Ero1 α with high activity also functions to regulate extracellular redox homeostasis.

Ero1 α is recognized as a cancer-associated oxidase because its expression is significantly elevated in many cancers such as breast (Kutomi *et al*, 2013), gastrointestinal (Battle *et al*, 2013), and pancreatic (Kukita *et al*, 2015) cancers. Moreover, Ero1 α enhances the expression of major histocompatibility complex class I antigen (Kukita *et al*, 2015), vascular endothelial growth factor (Tanaka *et al*, 2016), and programmed death-ligand 1 (Tanaka *et al*, 2017) via oxidative folding to promote tumor growth. Notably, Fam20C-dependent phosphorylation of secreted proteins is necessary for the proper adhesion, migration, and invasion of cancer cells (Tagliabracci *et al*, 2015). Therefore, future efforts to validate whether the p-Ero1 α levels are elevated in cancers and are correlated with a poor prognosis will greatly benefit the use of p-Ero1 α as a potential biomarker and a novel therapeutic target for various types of cancer.

Materials and Methods

Generation of constructs

The pGEX-6P-1 plasmids encoding human Ero1 α and pQE30-PDI were laboratory products (Zhang *et al*, 2014; Niu *et al*, 2016). The mutation of Ero1 α S145E was created using the Fast Mutagenesis System (TransGen). The expression of pcDNA3.1-Ero1 α -myc, pcDNA3.1-Ero1 α -HA, and/or pcDNA3.1-HA-ERp44 in mammalian cells was as previously described (Wang *et al*, 2014; Yang *et al*, 2016). pcDNA3.1-Ero1 α -HA-KDEL was generated by insertion of a KDEL motif between HA and the termination codon. pcDNA3.1-Ero1 α S145A and S145E with myc or HA tag were produced using the Fast Mutagenesis System (TransGen). pCCF-Fam20C-Flag and pCCF-Fam20C D478A-Flag were previously described (Tagliabracci *et al*, 2012). pcDNA3.1-roGFP-iE_{ER} was a kind gift from Dr. Christian Appenzeller-Herzog (University of Basel), and S30R, T39N, N105T, and I171V mutations were induced to generate the superfolded-roGFP-iE_{ER} as described elsewhere (Hoseki *et al*, 2016). All constructs were verified by DNA sequencing (Invitrogen).

Protein expression and purification

Recombinant full-length human Ero1 α proteins and PDI were expressed in *Escherichia coli* BL21 (DE3) cells and purified as before

(Wang *et al*, 2009). Maltose-binding protein (MBP) tagged human Fam20C protein (141–578) was expressed in Hi5 insect cells and purified from the conditioned medium, and the MBP tag was removed using gel filtration chromatography following tobacco etch virus protease digestion (Xiao *et al*, 2013). Proteins were quantified using the Bradford method with bovine serum albumin as a standard or spectrophotometrically at 280 nm and stored as aliquots at –80°C.

In vitro kinase assay

The reactions were initiated by adding ATP to a final concentration of 2 mM into buffer A (HEPES–NaOH, pH 7.0, 10 mM MnCl₂) containing 1 mg/ml recombinant Ero1 α and 20 μ g/ml purified Fam20C or Fam20C D478A protein at 30°C, and were terminated at different times by adding 20 mM EDTA. Proteins were separated by sodium dodecyl sulfate polyacrylamide gel electrophoresis (SDS–PAGE) and visualized by Coomassie Brilliant Blue staining and immunoblotting.

Oxygen consumption assay

Oxygen consumption was monitored at 25°C using an Oxygraph Clark-type oxygen electrode (Hansatech Instruments) as previously described (Wang *et al*, 2011). Reactions were initiated by adding Ero1 α proteins to a final concentration of 1 or 2 μ M into buffer B (100 mM Tris-HAc, pH 8.0, 50 mM NaCl, 2 mM EDTA) containing 1 mM dithiothreitol (DTT) or 20 μ M PDI proteins and 10 mM glutathione (GSH), respectively. For phosphorylated Ero1 α assay, reactions were initiated by adding 1 mM DTT or 20 mM GSH into buffer B with an *in vitro* kinase assay mixture containing 0.5 μ M Ero1 α or 1 μ M Ero1 α and 20 μ M PDI, respectively. Reaction rates were calculated by measuring the slope of the linear phase of the oxygen consumption curve.

Cell culture and transfection

HeLa cells were cultured in Dulbecco's modified Eagle's medium (Gibco), and HepG2 cells were cultured in RPMI 1640 medium (Gibco) supplemented with 10% fetal bovine serum (Gibco), 100 units/ml penicillin, and 100 μ g/ml streptomycin (Invitrogen) at 37°C with 5% CO₂. Plasmid transfection was accomplished by using Lipofectamine 2000 (Invitrogen) or ViaFect (Promega) according to the manufacturer's instructions. After 24–48 h, the transfected cells and culture medium were harvested for further analysis. For hypoxia treatment, cells were placed in a hypoxic chamber (BioSpherix) with 0.1% oxygen concentration for different period of time.

RNA interference

The pSUPER.retro.puro vector (Oligoengine) expressing the short-hairpin RNA (shRNA) targeting *FAM20C* sequence 5'-GAGCTG TACTCCAGACACA-3' was constructed according to the manufacturer's instructions. siERP44 with sequence 5'-UUAUUGC CGAGCUACUUCUUCUG-3' was obtained from GENEWIZ. HeLa cells were transfected with pSUPER plasmid by Lipofectamine 2000 or siRNA by RNAi-MAX (Invitrogen) on day 1, and co-transfected with the other plasmid on day 3. Cells and culture medium were harvested on day 4 for further analysis.

Mass spectrometry (MS)

Sample preparation

To identify the Fam20C interactome, HeLa cells were transfected with pcDNA4.0 or pcDNA4.0-Fam20C-Flag for 48 h, then harvested, and lysed. The cell extracts were incubated with anti-Flag M2 affinity gel (Sigma-Aldrich) overnight at 4°C with occasional vortexing. The immunoprecipitates were washed five times with ice-cold PBS. The proteins were then separated by SDS-PAGE and stained with Coomassie Brilliant Blue for MS analysis. For phosphorylation site identification, HeLa cells were transfected with pcDNA3.1-Ero1 α -HA for 24 h. The cell extracts were incubated with anti-HA (HA-7; Sigma-Aldrich) overnight, followed by addition of Agarose A+G (Beyotime). The immunoprecipitates were washed for five times, and the proteins were separated by SDS-PAGE gels, stained by Coomassie Brilliant Blue, and immunoblotted with anti-HA in parallel.

In-gel digestion of proteins

All gel bands excluding Fam20C and immunoglobulin chains were excised and cut into small plugs. After destaining, the gel plugs were reduced (10 mM DTT in 25 mM NH₄HCO₃ for 45 min at 56°C) and further alkylated (40 mM iodoacetamide in 25 mM NH₄HCO₃ for 45 min at room temperature in the dark). The plugs were washed twice with 50% acetonitrile in 25 mM NH₄HCO₃, dried using a SpeedVac, and digested with trypsin in 25 mM NH₄HCO₃ overnight at 37°C, followed by addition of formic acid to a 1% final concentration to terminate the reaction.

LC-MS/MS analysis

The digestion peptides were separated on a 75 μ m ID \times 20 cm C18 column packed with reversed-phase silica (Reprosil-Pur C18-AQ, 3 μ m; Dr. Maisch GmbH). A linear acetonitrile gradient was used to elute the bounded peptides, which were directly electrosprayed at a 2.0 kV voltage directly into a Q Exactive mass spectrometer (Thermo Fisher Scientific) equipped with a nano-liquid chromatography electrospray ionization source. In the data-dependent acquisition mode, the MS data were acquired at a high resolution of 70,000 (m/z 200) across a mass range of 300–1,600 m/z , followed by 20 tandem mass events on the top 20 precursor ions, which were isolated and fragmented in the HCD collision cell. Subsequently, MS/MS spectra were acquired at a resolution of 17,500 at m/z 200. The dynamic exclusion time was 40 s.

Protein identification

Database searches were performed on Proteome Discovery software, version 1.4 using SEQUEST HT search engine for protein identification and Percolator for false discovery rate (FDR, < 1%) analysis against a UniProt human protein database. The search parameters were set as follows: 10 ppm mass tolerance for precursor ions; 0.02 Da mass tolerance for product ions; two missed cleavage sites allowed for trypsin digestion. For Fam20C interactome identification, proteins (unique peptides \geq 2) were selected and protein interaction was defined as significant if the MS area ratio of Fam20C overexpressed group (B) to control group (A) is \geq 3. A total of 1,876 proteins were identified, of which 349 are localized in the ER and Golgi based on DAVID GO term analysis. For phosphorylation site identification, we selected phosphorylation for serine, threonine or

tyrosine and methionine oxidation as variable modifications, and the cysteine carbamidomethylation as a fixed modification. The peptides confidence was set as high for peptides filter. The tandem mass spectra of the matched phosphorylated peptides were manually checked for their validity.

Subcellular fractionation

Subcellular fractionation was performed as described (Wu *et al*, 2018). Briefly, the harvested HeLa cells were suspended in 20 mM Tricine (pH 7.8) and 250 mM sucrose containing protease inhibitor cocktail and phosphatase inhibitor cocktail and kept on ice for 20 min. The cells were homogenized before centrifugation at 3,000 \times g for 10 min to remove the nucleus and residual cells. The postnuclear supernatant was loaded on 30% Percoll and centrifuged at 144,200 \times g for 30 min in a Beckman SW41 Ti rotor. Fractionated samples were collected from top to bottom gently and subjected to SDS-PAGE and immunoblotting.

Immunoblotting

Harvested cells were lysed in radio immunoprecipitation assay (RIPA) lysis buffer (50 mM Tris-HCl, pH 7.4, 150 mM NaCl, 0.25% deoxycholic acid, 1% NP-40, 1 mM EDTA, Millipore) containing 1 mM phenylmethanesulfonyl fluoride (PMSF), phosphatase inhibitor cocktail (Roche), and protease inhibitor cocktail (Roche) for 30 min. The homogenate was centrifuged at 13,000 \times g for 15 min to remove cell debris. Protein quantification was performed using a BCA Kit (Beyotime). Culture medium was enriched by Concanavalin A (ConA, Sigma-Aldrich) at 4°C overnight, and the precipitates were washed three times before adding the loading buffer. Protein samples were analyzed by SDS-PAGE and then transferred to polyvinylidene difluoride (PVDF) membranes (Millipore) using a semi-dry transfer apparatus. The membranes were blocked in 5% milk (5% BSA for p-Ero1 α immunoblotting), incubated with antibodies and visualized by using a Chemi-Scope Mini imaging system (Clinx Science) with enhanced chemiluminescence (Thermo Fisher Scientific).

The following antibodies were used for immunoblotting: mouse monoclonal anti-Ero1 α (2G4, 1:1,000; Millipore), anti-PDI (RL90, 1:2,000; Abcam), anti-calnexin (610523, 1:500; BD Transduction), anti-GM130 (610822, 1:500; BD Transduction), anti-HIF1 α (NB100-105, 1:500; Novusbio), anti-Flag (M2, 1:2,000; Sigma-Aldrich), anti-myc (9E10, 1:5,000; Sigma-Aldrich), anti-HA (HA-7, 1:5,000; Sigma-Aldrich), anti-GAPDH (GAPDH-71.1, 1:50,000; Sigma-Aldrich); rabbit polyclonal anti-ERp44 (D17A6, 1:2,000; Cell Signaling Technology), anti-IRE1 α (14C10, 1:1,000; Cell Signaling Technology), anti-p-IRE1 α (EPR5253, 1:1,000; Abcam), anti-PERK (C33E10, 1:1,000; Cell Signaling Technology), anti-eIF2 α (D7D3, 1:1,000; Cell Signaling Technology), anti-p-eIF2 α (D7D3, 1:1,000; Cell Signaling Technology), goat anti-rabbit IgG (1:10,000; Sigma-Aldrich), and goat anti-mouse IgG (1:10,000; Sigma-Aldrich). Anti-p-Ero1 α recognizing pSer145 was purified from rabbit serum on immunization with a synthesized keyhole limpet hemocyanin (KLH)-conjugated peptide DESL(pS)EETQ-KAVLQC, and anti-Fam20C was purified from rabbit serum on immunization with a synthesized KLH-conjugated peptide CHSVVDDDLDTHEHAASAR.

Immunofluorescence

HepG2 cells were fixed with 4% formaldehyde for 15 min, permeabilized with 0.1% Triton X-100 for 5 min and blocked with 1% BSA for 30 min at room temperature. The cells were incubated with primary antibody and secondary antibody, each for 1 h. The antibodies used for immunofluorescence were as follows: anti-p-Ero1 α (1:50), anti-HA (1:500), anti-Flag (1:1,000), anti-PDI (1:500), anti-GM130 (1:250), goat anti-rabbit Alexa Fluor 488 (1:1,000; Invitrogen), goat anti-mouse Alexa Fluor 568 (1:1,000; Invitrogen). Hoechst 33258 (1:10,000; Sigma-Aldrich) was used to stain the nuclear DNA.

J-chain folding assay

J-chain folding assay was conducted as described (Wang *et al*, 2014). Myc-tagged human immunoglobulin J-chain (JcM) was co-expressed with Ero1 α -HA or Fam20C-Flag in HeLa cells for 24 h. Harvested cells were incubated with 10 mM DTT in DMEM at 37°C for 5 min to fully reduce JcM protein, instantly washed twice with ice-cold PBS to remove residual DTT, and re-suspended in DMEM at 20°C. Aliquots were taken and immediately blocked with 20 mM *N*-ethylmaleimide (NEM) at different time points. Cells were lysed in RIPA buffer containing 1 mM PMSF, phosphatase and protease inhibitor cocktails and 40 mM NEM. To observe the redox state of J-chain, the supernatants were resolved by non-reducing SDS-PAGE and visualized by immunoblotting with anti-myc.

Determination of ER redox with superfolded-roGFP-iE_{ER}

HeLa cells were transfected with superfolded-roGFP-iE_{ER} or co-transfected with Ero1 α -myc or Fam20C-Flag for 48 h. Harvested cells were washed twice in Hanks' balanced salt solution (HBSS; Gibco) and seeded onto a flat-bottom 96-well plate. The fluorescence intensities at 525 nm were measured with excitation at 390 and 465 nm, and the fluorescence ratio from excitation at 390 versus 465 nm was calculated.

λ -phosphatase assay

ConA precipitates from conditioned medium of HeLa cells transiently expressing Ero1 α were treated with 100 or 200 units λ -phosphatase (λ -PP; New England Biolabs) in 50 μ l buffer (50 mM HEPES, pH 7.5, 100 mM NaCl, 2 mM DTT, and 0.01% Brij 35) with 10 mM MnCl₂ at 30°C for 1 h, followed by immunoblotting.

Mouse mammary gland protein and RNA isolation

Mammary glands were taken from virgin or lactating C57BL/6 female mice at 14–17 weeks and homogenized in RIPA buffer containing 1 mM PMSF, phosphatase, and protease inhibitors cocktails with gentle stir in a microhomogenizer (Bio-gen Pro200). The homogenate was centrifuged at 13,000 \times g for 15 min, and the supernatant was mixed with a reducing loading buffer and analyzed by SDS-PAGE and immunoblotting. Total RNA was isolated from lactating or non-lactating mammary glands using TRIzol reagent (Invitrogen).

Quantitative real-time polymerase chain reaction (RT-qPCR)

RNA products were reverse-transcribed to cDNA using GoScript Reverse Transcription System (Promega). RT-qPCR was performed using SYBR Select Master Mix (Applied Biosystems) and QuantStudio 7 Flex machine (Applied Biosystems) according to the manufacturer's instructions. The expression level of the target genes was calculated as $2^{-\Delta\Delta CT}$ and normalized to that of *GAPDH*. All primers used are listed in Table EV1.

Generation of *FAM20C* knockout and *ERO1A* knockout HeLa cell lines by CRISPR/Cas9 genome editing

The 20-nt guide sequences targeting human *FAM20C* and *ERO1A* were designed using the clustered regularly interspaced short palindromic repeats (CRISPR) design tool at www.genome-engineering.org/crispr and cloned into the expression vector pSpCas9(BB)-2A-GFP (PX458) containing human codon optimized Cas9, the RNA components, and GFP (a gift from Feng Zhang, Addgene plasmid # 48138).

The guide sequences targeting exon 1 of human *FAM20C* and human *ERO1A* are shown below.

FAM20C

5'-GGGCTGCGCGCACGAACAGC-3' (clone 3 and 5)

ERO1A

5'-CAAACAAGAATCCCCAGCCG-3' (clone 10 and 12)

HeLa cells were transfected with pSpCas9(BB)-2A-GFP vector containing the single-guide RNAs (sgRNAs) by Viafect for 48 h, and GFP-positive cells were single-cell-sorted by fluorescence-activated cell sorting (BD Influx) into a 96-well plate format into DMEM supplemented with 10% FBS. Expanded single clones were screened for Fam20C and Ero1 α by protein immunoblotting. Genomic DNA (gDNA) was purified from clones using the TransDirect Animal Tissue PCR Kit (TransGen), and the region surrounding the protospacer adjacent motif (PAM) was amplified using the following primers.

FAM20C.

Forward: 5'-CGCGCGCCATGAAGATGAT-3'

Reverse: 5'-TTCTCCAGCGAGTGGGACGAGAGGT-3'

ERO1A.

Forward: 5'-GATCGCTGAGAGGCAGGA-3'

Reverse: 5'-AGAAGCACCTCTGTGCCG-3'

PCR products were purified using a gel extraction kit (Omega) and cloned into pEASY-T5 Zero cloning vector (TransGen). To determine the indels of individual alleles, eight to 16 bacterial colonies were expanded and the plasmid DNA was purified and sequenced (Invitrogen).

Circular dichroism spectroscopy

Circular dichroism spectrum of 0.2 mg/ml recombinant Ero1 α WT or Ero1 α S145E in 50 mM sodium phosphate buffer (pH 7.0) was measured from 190 to 260 nm at 25°C by Chirascan Plus (Applied Photophysics). Scanning speed was 2.5 s/dot.

Intrinsic fluorescence assay

Fluorescence spectrum of 2 μ M recombinant Ero1 α WT or Ero1 α S145E in protein store buffer (50 mM Tris-HCl, pH 7.6, 150 mM

NaCl, 2 mM EDTA) from 305 to 405 nm was measured with excitation at 295 nm at 25°C using Hitachi F7000. Scanning speed was 60 nm/min.

Ero1 α activation assay

Recombinant Ero1 α C99A/C104A/C166A or Ero1 α C99A/C104A/C166A/S145E was incubated with 50 mM potassium ferricyanide for 1 h at 25°C to prepare the oxidized Ero1 α protein. After chromatography, 1 μ M monomeric oxidized Ero1 α was mixed with 10 μ M reduced PDI, and aliquots were taken at indicated times and immediately quenched with 20 mM NEM.

Ethics

Animal experiments were conducted with the approval of the Institutional Biomedical Research Ethics Committee of the Institute of Biophysics, Chinese Academy of Science.

Data availability

The mass spectrometry proteomics data have been deposited to the ProteomeXchange Consortium via the PRIDE (Vizcaino *et al*, 2016) partner repository with the dataset identifier PXD009333.

Expanded View for this article is available online.

Acknowledgements

We acknowledge Junjie Hu and Yanfang Wu for assisting in subcellular fractionation, Likun Wang for providing a hypoxic chamber, Yuhao Gao, Junjie Hou, Jingqi Fang, Yunpeng Zhai, Mengmeng Zhang, and Yan Teng for technical assistance. This work was supported by National Key R&D Program of China (2016YFA0500200, 2017YFA0504000), National Natural Science Foundation of China (31571163, 31771261, 31370758), and Youth Innovation Promotion Association CAS to LW and XW.

Author contributions

LW conceived the project. JZ, JX, CCW, and LW designed research; JZ, QZ, XEW, JY, XC, JW, and XW performed research; JZ, JX, and LW analyzed data; JZ, CCW, and LW wrote the paper.

Conflict of interest

The authors declare that they have no conflict of interest.

References

- Anelli T, Alessio M, Bachi A, Bergamelli L, Bertoli G, Camerini S, Mezghrani A, Ruffato E, Simmen T, Sitia R (2003) Thiol-mediated protein retention in the endoplasmic reticulum: the role of Erp44. *EMBO J* 22: 5015–5022
- Anelli T, Bergamelli L, Margittai E, Rimessi A, Fagioli C, Malgaroli A, Pinton P, Ripamonti M, Rizzuto R, Sitia R (2012) Ero1 alpha regulates Ca²⁺ fluxes at the endoplasmic reticulum-mitochondria interface (MAM). *Antioxid Redox Signal* 16: 1077–1087
- Appenzeller-Herzog C, Riemer J, Christensen B, Sorensen ES, Ellgaard L (2008) A novel disulphide switch mechanism in Ero1 alpha balances ER oxidation in human cells. *EMBO J* 27: 2977–2987
- Baker KM, Chakravarthi S, Langton KP, Sheppard AM, Lu H, Bulleid NJ (2008) Low reduction potential of Ero1 alpha regulatory disulphides ensures tight control of substrate oxidation. *EMBO J* 27: 2988–2997
- Battle DM, Gunasekara SD, Watson GR, Ahmed EM, Saysell CG, Altaf N, Sanusi AL, Munipalle PC, Scoones D, Walker J, Viswanath Y, Benham AM (2013) Expression of the endoplasmic reticulum oxidoreductase Ero1 alpha in gastro-intestinal cancer reveals a link between homocysteine and oxidative protein folding. *Antioxid Redox Signal* 19: 24–35
- Birk J, Meyer M, Aller I, Hansen HG, Odermatt A, Dick TP, Meyer AJ, Appenzeller-Herzog C (2013) Endoplasmic reticulum: reduced and oxidized glutathione revisited. *J Cell Sci* 126: 1604–1617
- Cabibbo A, Pagani M, Fabbri M, Rocchi M, Farmery MR, Bulleid NJ, Sitia R (2000) ERO1-L, a human protein that favors disulfide bond formation in the endoplasmic reticulum. *J Biol Chem* 275: 4827–4833
- Chin K, Kang G, Qu J, Gardner LB, Coetzee WA, Zito E, Fishman GI, Ron D (2011) The sarcoplasmic reticulum luminal thiol oxidase ERO1 regulates cardiomyocyte excitation-coupled calcium release and response to hemodynamic load. *FASEB J* 25: 2583–2591
- Cohen P (2002) The origins of protein phosphorylation. *Nat Cell Biol* 4: E127–E130
- Cui J, Xiao J, Tagliabracci VS, Wen J, Rahdar M, Dixon JE (2015) A secretory kinase complex regulates extracellular protein phosphorylation. *eLife* 4: e06120
- Delaunay-Moisan A, Ponsoero A, Toledano MB (2017) Reexamining the function of glutathione in oxidative protein folding and secretion. *Antioxid Redox Signal* 27: 1178–1199
- Fass D, Thorpe C (2018) Chemistry and enzymology of disulfide cross-linking in proteins. *Chem Rev* 118: 1169–1198
- Gilady SY, Bui M, Lynes EM, Benson MD, Watts R, Vance JE, Simmen T (2010) Ero1 alpha requires oxidizing and normoxic conditions to localize to the mitochondria-associated membrane (MAM). *Cell Stress Chaperones* 15: 619–629
- Gross E, Kastner DB, Kaiser CA, Fass D (2004) Structure of Ero1p, source of disulfide bonds for oxidative protein folding in the cell. *Cell* 117: 601–610
- Gross E, Sevier CS, Heldman N, Vitu E, Bentzur M, Kaiser CA, Thorpe C, Fass D (2006) Generating disulfides enzymatically: reaction products and electron acceptors of the endoplasmic reticulum thiol oxidase Ero1p. *Proc Natl Acad Sci USA* 103: 299–304
- Hammarsten O (1883) Zur frage ob casein ein einheitlicher stoff sei. *Hoppe Seylers Z Physiol Chem* 7: 227–273
- Hogg PJ (2003) Disulfide bonds as switches for protein function. *Trends Biochem Sci* 28: 210–214
- Hoseki J, Oishi A, Fujimura T, Sakai Y (2016) Development of a stable ERroGFP variant suitable for monitoring redox dynamics in the ER. *Biosci Rep* 36: e00316
- Inaba K, Masui S, Iida H, Vavassori S, Sitia R, Suzuki M (2010) Crystal structures of human Ero1 alpha reveal the mechanisms of regulated and targeted oxidation of PDI. *EMBO J* 29: 3330–3343
- Ishikawa HO, Xu A, Ogura E, Manning G, Irvine KD (2012) The Raine syndrome protein Fam20C is a Golgi kinase that phosphorylates biomineralization proteins. *PLoS ONE* 7: e42988
- Kim S, Sideris DP, Sevier CS, Kaiser CA (2012) Balanced Ero1 activation and inactivation establishes ER redox homeostasis. *J Cell Biol* 196: 713–725
- Kukita K, Tamura Y, Tanaka T, Kajiwara T, Kutomi G, Saito K, Okuya K, Takaya A, Kanaseki T, Tsukahara T, Hirohashi Y, Torigoe T, Furuhashi T, Hirata K, Sato N (2015) Cancer-associated oxidase ERO1-alpha regulates the

- expression of MHC class I molecule via oxidative folding. *J Immunol* 194: 4988–4996
- Kutomi G, Tamura Y, Tanaka T, Kajiwara T, Kukita K, Ohmura T, Shima H, Takamaru T, Satomi F, Suzuki Y, Torigoe T, Sato N, Hirata K (2013) Human endoplasmic reticulum oxidoreductin 1- α is a novel predictor for poor prognosis of breast cancer. *Cancer Sci* 104: 1091–1096
- Li G, Mongillo M, Chin KT, Harding H, Ron D, Marks AR, Tabas I (2009) Role of ERO1- α -mediated stimulation of inositol 1,4,5-triphosphate receptor activity in endoplasmic reticulum stress-induced apoptosis. *J Cell Biol* 186: 783–792
- Marino M, Stoilova T, Giorgi C, Bachi A, Cattaneo A, Auricchio A, Pinton P, Zito E (2015) SEPN1, an endoplasmic reticulum-localized selenoprotein linked to skeletal muscle pathology, counteracts hyperoxidation by means of redox-regulating SERCA2 pump activity. *Hum Mol Genet* 24: 1843–1855
- May D, Itin A, Gal O, Kalinski H, Feinstein E, Keshet E (2005) Ero1-L α plays a key role in a HIF-1-mediated pathway to improve disulfide bond formation and VEGF secretion under hypoxia: implication for cancer. *Oncogene* 24: 1011–1020
- Mezghrani A, Fassio A, Benham A, Simmen T, Braakman I, Sitia R (2001) Manipulation of oxidative protein folding and PDI redox state in mammalian cells. *EMBO J* 20: 6288–6296
- Niu Y, Zhang L, Yu J, Wang CC, Wang L (2016) Novel roles of the non-catalytic elements of yeast protein-disulfide isomerase in its interplay with endoplasmic reticulum oxidoreductin 1. *J Biol Chem* 291: 8283–8294
- Pollak AJ, Haghighi K, Kunduri S, Arvanitis DA, Bidwell PA, Liu G, Singh VP, Gonzalez DJ, Sanoudou D, Wiley SE, Dixon JE, Kranias EG (2017) Phosphorylation of serine96 of histidine-rich calcium-binding protein by the Fam20C kinase functions to prevent cardiac arrhythmia. *Proc Natl Acad Sci USA* 114: 9098–9103
- Raine J, Winter RM, Davey A, Tucker SM (1989) Unknown syndrome: microcephaly, hypoplastic nose, exophthalmos, gum hyperplasia, cleft-palate, low set ears, and osteosclerosis. *J Med Genet* 26: 786–788
- Ramming T, Appenzeller-Herzog C (2012) The physiological functions of mammalian endoplasmic oxidoreductin 1: on disulfides and more. *Antioxid Redox Signal* 16: 1109–1118
- Sevier CS, Qu H, Heldman N, Gross E, Fass D, Kaiser CA (2007) Modulation of cellular disulfide-bond formation and the ER redox environment by feedback-regulation of Ero1. *Cell* 129: 333–344
- Sevier CS, Kaiser CA (2008) Ero1 and redox homeostasis in the endoplasmic reticulum. *Biochim Biophys Acta-Mol Cell Res* 1783: 549–556
- Tagliabracci VS, Engel JL, Wen J, Wiley SE, Worby CA, Kinch LN, Xiao J, Grishin NV, Dixon JE (2012) Secreted kinase phosphorylates extracellular proteins that regulate biomineralization. *Science* 336: 1150–1153
- Tagliabracci VS, Pinna LA, Dixon JE (2013) Secreted protein kinases. *Trends Biochem Sci* 38: 121–130
- Tagliabracci VS, Wiley SE, Guo X, Kinch LN, Durrant E, Wen J, Xiao J, Cui J, Nguyen KB, Engel JL, Coon JJ, Grishin N, Pinna LA, Pagliarini DJ, Dixon JE (2015) A single kinase generates the majority of the secreted phosphoproteome. *Cell* 161: 1619–1632
- Tanaka T, Kutomi G, Kajiwara T, Kukita K, Kochin V, Kanaseki T, Tsukahara T, Hirohashi Y, Torigoe T, Okamoto Y, Hirata K, Sato N, Tamura Y (2016) Cancer-associated oxidoreductase ERO1- α drives the production of VEGF via oxidative protein folding and regulating the mRNA level. *Br J Cancer* 114: 1227–1234
- Tanaka T, Kutomi G, Kajiwara T, Kukita K, Kochin V, Kanaseki T, Tsukahara T, Hirohashi Y, Torigoe T, Okamoto Y, Hirata K, Sato N, Tamura Y (2017) Cancer-associated oxidoreductase ERO1- α promotes immune escape through up-regulation of PD-L1 in human breast cancer. *Oncotarget* 8: 24706–24718
- Tu BP, Weissman JS (2002) The FAD- and O(2)-dependent reaction cycle of Ero1-mediated oxidative protein folding in the endoplasmic reticulum. *Mol Cell* 10: 983–994
- Tu BP, Weissman JS (2004) Oxidative protein folding in eukaryotes: mechanisms and consequences. *J Cell Biol* 164: 341–346
- Vavassori S, Cortini M, Masui S, Sannino S, Anelli T, Caserta IR, Fagioli C, Mossuto MF, Fornili A, van Anken E, Degano M, Inaba K, Sitia R (2013) A pH-regulated quality control cycle for surveillance of secretory protein assembly. *Mol Cell* 50: 783–792
- Vitu E, Kim S, Sevier CS, Lutzky O, Heldman N, Bentzur M, Unger T, Yona M, Kaiser CA, Fass D (2010) Oxidative activity of yeast Ero1p on protein disulfide isomerase and related oxidoreductases of the endoplasmic reticulum. *J Biol Chem* 285: 18155–18165
- Vizcaino JA, Csordas A, Del-Toro N, Dianas JA, Griss J, Lavidas I, Mayer G, Perez-Riverol Y, Reisinger F, Ternent T, Xu QW, Wang R, Hermjakob H (2016) 2016 update of the PRIDE database and its related tools. *Nucleic Acids Res* 44: 11033
- Wang L, Wang L, Vavassori S, Li S, Ke H, Anelli T, Degano M, Ronzoni R, Sitia R, Sun F, Wang CC (2008) Crystal structure of human ERp44 shows a dynamic functional modulation by its carboxy-terminal tail. *EMBO Rep* 9: 642–647
- Wang L, Li S, Sidhu A, Zhu L, Liang Y, Freedman RB, Wang CC (2009) Reconstitution of human Ero1-L α /protein-disulfide isomerase oxidative folding pathway *in vitro*. Position-dependent differences in role between the a and a' domains of protein-disulfide isomerase. *J Biol Chem* 284: 199–206
- Wang L, Zhu L, Wang CC (2011) The endoplasmic reticulum sulfhydryl oxidase Ero1 beta drives efficient oxidative protein folding with loose regulation. *Biochem J* 434: 113–121
- Wang L, Zhang L, Niu Y, Sitia R, Wang CC (2014) Glutathione peroxidase 7 utilizes hydrogen peroxide generated by Ero1 α to promote oxidative protein folding. *Antioxid Redox Signal* 20: 545–556
- Wang L, Wang X, Wang CC (2015) Protein disulfide-isomerase, a folding catalyst and a redox-regulated chaperone. *Free Radic Biol Med* 83: 305–313
- Wu Y, Li X, Jia J, Zhang Y, Li J, Zhu Z, Wang H, Tang J, Hu J (2018) Transmembrane E3 ligase RNF183 mediates ER stress-induced apoptosis by degrading Bcl-xL. *Proc Natl Acad Sci USA* 115: E2762–E2771
- Xiao J, Tagliabracci VS, Wen J, Kim SA, Dixon JE (2013) Crystal structure of the Golgi casein kinase. *Proc Natl Acad Sci USA* 110: 10574–10579
- Yang K, Li DF, Wang X, Liang J, Sitia R, Wang CC, Wang X (2016) Crystal structure of the ERp44-peroxiredoxin 4 complex reveals the molecular mechanisms of thiol-mediated protein retention. *Structure* 24: 1755–1765
- Zhang L, Niu Y, Zhu L, Fang J, Wang X, Wang L, Wang CC (2014) Different interaction modes for protein-disulfide isomerase (PDI) as an efficient regulator and a specific substrate of endoplasmic reticulum oxidoreductin-1 α (Ero1 α). *J Biol Chem* 289: 31188–31199